Available online at www.sciencedirect.com
ScienceDirect
Annals of Physics 323 (2008) 337–355
ANNALS of PHYSICS
www.elsevier.com/locate/aop

Confinement of monopole field lines in a superconductor at $T \neq 0$

Marco Cardoso [a,b,c], Pedro Bicudo [a,b], Pedro D. Sacramento [a,c,*]

[a] *Departamento de Física, Instituto Superior Técnico, Universidade Técnica de Lisboa, Av. Rovisco Pais, 1049-001 Lisboa, Portugal*
[b] *Centro de Física Teórica de Partículas, Instituto Superior Técnico, Universidade Técnica de Lisboa, Av. Rovisco Pais, 1049-001 Lisboa, Portugal*
[c] *Centro de Física das Interacções Fundamentais, Instituto Superior Técnico, Universidade Técnica de Lisboa, Av. Rovisco Pais, 1049-001 Lisboa, Portugal*

Received 8 February 2007; accepted 22 February 2007
Available online 12 March 2007

Abstract

We apply the Bogoliubov-de Gennes equations to the confinement of a monopole–antimonopole pair in a superconductor. This is related to the problem of a quark–antiquark pair bound by a confining string, consisting of a colour-electric flux tube, dual to the magnetic vortex of type-II superconductors. We study the confinement of the field lines due to the superconducting state and calculate the effective potential between the two monopoles. The monopoles can be simulated in a real experiment inserting two long and thin magnetic rods. At short distances the potential is Coulombic and at large distances the potential is linear, as previously determined solving the Ginzburg–Landau equations. The magnetic field lines and the string tension are also studied as a function of the temperature T. Because we take into account the explicit fermionic degrees of freedom, this work may open new perspectives to the breaking of chiral symmetry or to colour superconductivity.

Keywords: Confinement; Monopoles–antimonopoles; Superconductors; Meissner effect; Flux tube

* Corresponding author. Address: Centro de Física das Interacções Fundamentais, Instituto Superior Técnico, Universidade Técnica de Lisboa, Av. Rovisco Pais, 1049-001 Lisboa, Portugal. Fax: +351 21 8419143.
E-mail address: pdss@cfif.ist.utl.pt (P.D. Sacramento).

0003-4916/$ - see front matter
doi:10.1016/j.aop.2007.02.007

1. Introduction

Right after QCD was proposed as the theory of strong interactions [1,2], different ideas for QCD confinement were inspired in the magnetic confinement in superconductors. Here we study a condensed matter problem, the confinement in a superconductor of electromagnetic field lines produced by a monopole–antimonopole pair. Although this is not a QCD problem, we address it with a perspective similar to QCD studies of the confinement of the color fields produced by a quark–anriquark pair.

The confinement of magnetic field lines in superconductors occurs through an Anderson–Higgs mechanism such that the photons of the electromagnetic field acquire a mass and are therefore exponentially damped in the superconductor. This constitutes the Meissner effect discovered experimentally in 1933. Indeed, at the boundary between the exterior and the superconductor, the parallel component of the external magnetic field is damped inside the superconductor on a scale λ, the penetration length. In this work we consider that the magnetic field lines in the superconductor emerge (converge) from (to) a monopole (antimonopole) inserted in the bulk of the superconductor. A possible way to achieve this is through the insertion of two thin and long magnetic rods of opposite magnetizations. When the distance d between the monopole and the antimonopole is smaller than λ, the Coulomb interaction is dominant. When $d \gg \lambda$, the linear interaction, characterized by the string tension σ, is preponderant. This is schematically shown in Fig. 1. Another relevant scale in a superconductor is the coherence length, defined as the distance over which the superconducting order parameter (pair density) acquires its bulk value. The ratio of these two lengths determines the magnetic properties of the superconductor: for $k = \lambda/\xi < 1/\sqrt{2}$ the superconductor is of type-I, a complete Meissner effect is observed and the magnetic field is completely expelled from the superconductor (perfect diamagnet) over a distance defined by the penetration length. If $k = \lambda/\xi > 1/\sqrt{2}$ the superconductor is of type-II and the magnetic field penetrates in the material through quantized vortices, whose density increases until their cores (with size given by the coherence length) overlap and the system becomes normal.

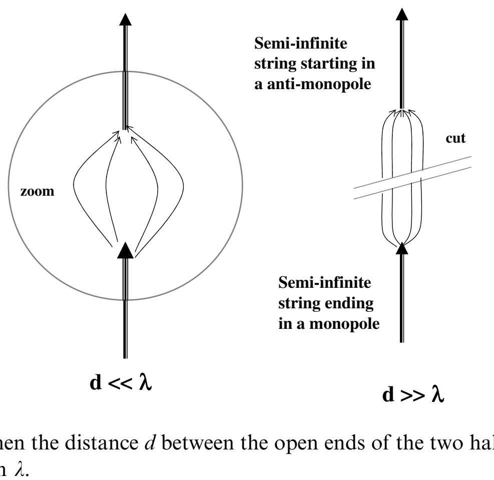

Fig. 1. The magnetic field when the distance d between the open ends of the two half strings is respectively much smaller and much larger than λ.

The confining string is an important candidate to solve the confinement problem of quantum chromodynamics (QCD). Nielsen and Olesen [3] suggested that the magnetic flux tube vortex of type-II superconductors could be applied, after a dual transformation, to colour-electric flux tube strings [4] in QCD. Soon afterwards Nambu [5], 't Hooft [6], and Mandelstam [7] developed the thesis that the open colour-electric string was able to confine quark–anriquark systems, where the quark–anriquark pair is dual to a Dirac [8] monopole–antimonopole pair. This idea was further developed by Baker, Ball and Zachariasen [9,10] and co-authors, who developed dual QCD, and also studied systems similar to a monopole–antimonopole pair in a superconductor in the Ginzburg–Landau framework. At the onset of QCD, lattice QCD was also developed by Wilson [11], who showed analytically that the strong coupling limit of QCD is equivalent to a string theory. The study of strings at the realistic transition between the strong and weak coupling of Lattice QCD was further explored by several authors. Bali [12,13] and Polikarkov [14,15] and co-authors studied in detail the string formation between static quark–anriquark sources in Lattice QCD. Importantly, colour superconductivity was also proposed to exist at finite baryon density by Alford, Rajagopal and Wilczek [16].

One should mention that QCD differs from type-II superconductors in many details. Baker, Ball and Zachariasen found that dual QCD is at the frontier between type-I and type-II superconductivity. The spin dependence of the quark–anriquark interaction, with no correspondance in the monopole–antimonopole interaction, was also addressed by De Rujula, Georgi and Glashow, and [17] Henriques, Kellett and Moorhouse [18] identified the role of the confining string in the spin dependent interactions. Moreover Takahashi, Suganuma and co-authors [19,20] also studied the three-legged string formation between three static quark sources, proposed to exist in Baryons. It is clear that this needs a SU(3) symmetry, unlike in type-I or type-II superconductors. Okiharu, Suganuma and Takahashi [21,22], further studied the tetraquark and pentaquark potentials. The idea of bag model, separating the interior of the flux tube from the remaining of the universe, was developed by Chodos, Jaffe, Johnson, Thorn and Weisskopf [23], and this lead Jaffe and Johnson to propose the existence of exotic hadrons, including glueballs, needing also a SU(3) symmetry, [24]. Moreover, many problems in QCD confinement with strings remain to be solved. For instance in the limit of infinitely thin relativistic strings [25], the world sheet swept out by a string in space time can only be quantized in 26 dimensions. For example light quarks, which condense the vacuum with chiral symmetry spontaneously breaking $^3P0$ scalar quark–anriquark pairs described by Bicudo and Ribeiro [26], are not yet fully compatible with string confinement. These problems, and other open problems of QCD confinement, motivate very interesting and active investigations.

Nevertheless the main condensed matter inspiration of QCD confinement, the pair of a monopole and a antimonopole in a superconductor, remains to be fully explored. Many years ago, Ball and Caticha [27], already studied the monopole–antimonopole pair in Ginzburg–Landau type-I and type-II superconductors. The Ginzburg–Landau superconductivity can be compared to pure gauge QCD, where fermions are absent. However, the new data on heavy-ion collisions and on dense quark stars motivates the interest both in finite temperature and in finite fermion density QCD. While in the full QCD case the fermions may already need to be considered due to chiral symmetry breaking and to the coupling of quarks to gluons, it is clear that in dense quark stars, where colour superconductivity may occur, the fermions cannot be ignored. In this paper we apply the Bogoliubov-de Gennes (BdG) equations, enabling a microscopic understanding of the role of electronic states in the confinement of magnetic and electric fields in superconductors. Moreover we address the effect of finite temperature in the magnetic confinement. We hope that this model may also be inspirational to QCD.

We are interested in the geometric configuration where two solenoids or magnetic rods, with opposite poles, and with one quantum of inner magnetic flux, are inserted in a superconductor. We assume that the other end of each solenoid or magnetic rod is very distant and plays no role here. In the limit of very thin solenoids, each solenoid is equivalent to a magnetic monopole (or antimonopole) plus its associated Dirac string introduced to satisfy Maxwell's equation $\nabla \cdot \mathbf{B} = 0$. The produced external magnetic field of this is identical through a gauge transformation to the one of the Ball and Caticha geometric choice, where a single string directly links the monopole and the anti-monopole. We choose our configuration, depicted in Fig. 1 because it is in principle amenable to an experimental setup, where the magnetic confining force may eventually be measured. The plausible experiment consists in a superconductor, where an extremely thin hole has been drilled, allowing the also extremely thin solenoids or magnetic rods to move inside the superconductor. The confining force should then be measurable at the other ends of the extremely thin solenoids or magnetic rods, when the respective magnetization is maintained during the experiment. Nanorods with diameters of the order of 1–10 nm may be achieved [28] in a way similar to metallic rods that have been inserted in a polymer or silicon matrix [29]. These diameters are small compared to both the coherence length and especially the penetration length in type-II superconductors, which typically vary between 1–100 and 60–1000 nm, respectively.

The problem of the quasi-particle states due to the presence of a vortex in a s-wave superconductor was solved long ago both analytically [30] and numerically [31]. There are bound states localized in the vicinity of the vortex location and a continuum of delocalized states. Classifying the states in terms of the angular momentum around the vortex line, allowed to determine that there is a branch of boundstates, one for each angular momentum value [31]. The results were obtained looking for an order parameter of the form $\Delta = \Delta_0 e^{-in\varphi}$ where φ is the polar angle and n fixes the vorticity, chosen originally as $n = 1$. The core states are coherent superpositions of particle and hole states and interpreted as being the result of constructive interference of multiple Andreev scattering from the spatial variation of the order parameter [32]. The case of zero vorticity, $n = 0$, corresponds to the absence of a vortex.

The vortex lines in general appear due to the application of an external magnetic field typically homogeneous. However, we can as well consider the presence of magnetic field lines that are due to a solenoid or a magnetic rod inserted in the superconductor. Actually, the magnetic field lines do not need to penetrate the superconductor itself, since what really matters is the vector potential. It is the vector potential that appears in the Hamiltonian of the system in the presence of a magnetic field [33], as is well known. This has been emphasized [34] considering a superconductor in the form of a cylindrical shell of internal radius R and width a in the center of which is inserted either a solenoid or a magnetic rod of radius r smaller than R. In these systems, considering the length of the cylinders very large compared to the radius, the field lines will close far from the supercondutor and therefore no field lines penetrate the cylinder. However, the vector potential due to the flux contained in the transverse section is non-zero and the field has the same effect on the supercurrents.

Recently it was stressed that the important characteristic that determines the boundstates is the winding of the phase [35]. The detailed form of the order parameter in the vicinity of the vortex core is not so relevant. Performing a non-self-consistent study of the spectrum it was found that the suppression of the gap function has a minor role. The supercurrent acts in non-symmetrical way on the particle and hole parts of the quasiparticles. It tends to decrease the angular momentum of the particle part and to increase the angular momentum of the hole part.

A fully self-consistent solution of the influence of a very long solenoid on the properties of a superconductor was addressed in Ref. [36]. The internal field originated in the supercurrents must adjust itself to the solution chosen according to the external field exerted by the solenoid. The total magnetic flux was fully determined by the choice of the angular momentum of the gap function and the value of n determines the vorticity of the vortex solution. Depending on the relation of the value of n and the value of the external field, the internal currents create fields that compensate, undercompensate or overcompensate the external field. The various situations lead to different spectral structures depending on the width of the solenoid. These in turn originate different structures for the internal field and supercurrents generated. The limit of a very thin solenoid, similar in nature to a Dirac string, is qualitatively different. It was shown that when the vorticity chosen equals the unit of external flux the currents generated vanish and no bound states appear. Otherwise the currents may be positive, and branches of boundstates with positive energies appear, or the currents are negative, and branches of negative energies appear. These results confirmed the link between the boundstates and the internal currents in a self-consistent way. In the case of a finite width solenoid the number of boundstates equals the vorticity of the gap function and is insensitive to the external field. The results can also describe a magnetic dot superimposed on the superconductor if in addition to the magnetic field due to the dot one applies an external homogeneous field. In this case the external field compensates the returning field lines due to the dot [37] that would appear away from the dot position, eliminating anti-vortices in the superconductor. The more complex and realistic case of a magnetic rod inserted in the superconductor was also considered but we will limit ourselves in this work to the very thin limit, to establish a closer link to the confinement of the monopole–antimonopole flux tube.

Here we study monopole–antimonopole confinement in a superconductor with finite fermion density and finite temperatures. The BdG framework, applied to the monopole–antimonopole pair is detailed in Section 2. In Section 3 we show the results at $T = 0$, and compare them with the Ball-Caticha paper. In Section 4 we show the results at $T \neq 0$. In Section 5 we conclude.

2. Bogoliubov de Gennes equations and the monopole–antimonopole field

2.1. Fermion pairing

Consider a fermionic system with an effective attractive interaction between the particles defined by an Hamiltonian

$$\begin{aligned} H = & \int \mathrm{d}\mathbf{r} \sum_{\sigma} c^{\dagger}(\mathbf{r},\sigma) \frac{\left(\mathbf{p} - \frac{e}{c}\mathbf{A}\right)^2}{2m} c(\mathbf{r},\sigma) \\ & - \frac{1}{2} g \int \mathrm{d}\mathbf{r} \sum_{\sigma,\sigma'} c^{\dagger}(\mathbf{r},\sigma) c^{\dagger}(\mathbf{r},\sigma') c(\mathbf{r},\sigma') c(\mathbf{r},\sigma) \end{aligned} \tag{1}$$

where $c^{\dagger}(\mathbf{r},\sigma)$ creates a fermion at site $\mathbf{r}$ with spin σ. $\mathbf{A}$ is the vector potential. In BCS theory, this leads to fermion–fermion and antifermion–antifermion pairing. Defining the field of a pair as $\Delta(\mathbf{r})$, and considering a conventional s-wave superconductor, the Hamiltonian is decoupled like

$$\begin{aligned} H_{\mathrm{BCS}} = &\int \mathrm{d}\mathbf{r} \sum_{\sigma} c^{\dagger}(\mathbf{r},\sigma)\left[\frac{\left(\mathbf{p}-\frac{e}{c}\mathbf{A}\right)^2}{2m} - E_{\mathrm{F}}\right] c(\mathbf{r},\sigma) \\ &+ \int \mathrm{d}\mathbf{r}[\Delta(\mathbf{r})c^{\dagger}(\mathbf{r},\uparrow)c^{\dagger}(\mathbf{r},\downarrow) + \Delta^{*}(\mathbf{r})c(\mathbf{r},\downarrow)c(\mathbf{r},\uparrow)] \end{aligned} \tag{2}$$

Here E_{F} is the Fermi energy. The Hamiltonian is diagonalized through a canonical transformation

$$\begin{aligned} c(\mathbf{r},\uparrow) &= \sum_i (u_i(\mathbf{r})\gamma_{i,\uparrow} - v_i^{*}(\mathbf{r})\gamma_{i,\downarrow}^{\dagger}) \\ c(\mathbf{r},\downarrow) &= \sum_i (u_i(\mathbf{r})\gamma_{i,\downarrow} + v_i^{*}(\mathbf{r})\gamma_{i,\uparrow}^{\dagger}) \end{aligned} \tag{3}$$

Here the fermionic operators $\gamma_{i,\sigma}$ annihilate a quasiparticle in the level i and with spin σ. Defining the diagonalized Hamiltonian as

$$H = E_{\mathrm{g}} + \sum_{i,\sigma} E_i \gamma_{i,\sigma}^{\dagger}\gamma_{i,\sigma} \tag{4}$$

where E_{g} is the groundstate energy, the physical meaning of the new operators is that they create the excitations of the system, and therefore we must restrict ourselves to the positive energies. Using the commutation relations of the operators with the Hamiltonian leads to the Bogoliubov-de Gennes equations (BdG) [33] for the amplitudes $u(\mathbf{r})$ and $v(\mathbf{r})$:

$$\left(\frac{1}{2m}\left(\mathbf{p}-\frac{e}{c}\mathbf{A}\right)^2 - E_{\mathrm{F}}\right)u_i(\mathbf{r}) + \Delta(\mathbf{r})v_i(\mathbf{r}) = E_i u_i(\mathbf{r}) \tag{5}$$

$$-\left(\frac{1}{2m}\left(\mathbf{p}+\frac{e}{c}\mathbf{A}\right)^2 - E_{\mathrm{F}}\right)v_i(\mathbf{r}) + \Delta^{*}(\mathbf{r})u_i(\mathbf{r}) = E_i v_i(\mathbf{r}) \tag{6}$$

$\mathbf{A}(\mathbf{r})$ is the vector potential, $\Delta(\mathbf{r})$ is the pairing function given by

$$\Delta(\mathbf{r}) = g \sum_{0<E_i\leqslant\hbar\omega_{\mathrm{D}}} u_i(\mathbf{r})v_i^{*}(\mathbf{r})(1-2f(E_i)). \tag{7}$$

Here $f(E_i)$ is the Fermi–Dirac distribution given by

$$f(E_i) = \frac{1}{e^{\frac{E_i}{k_{\mathrm{B}}T}} + 1} \tag{8}$$

where T is the temperature, assumed smaller than the critical temperature T_{c}, below which superconductivity arises. The pairing between the electrons occurs on an energy scale $\hbar\omega_{\mathrm{D}}$, called the Debye energy. In conventional superconductors this is the cutoff energy provided by the phonon exchange between electrons. An example of electronic wavefunctions u and v obtained in this paper is depicted in Fig. 2.

Let us take the order parameter in the form

$$\Delta(\mathbf{r}) = \Delta(\rho,z)e^{-in\varphi} \tag{9}$$

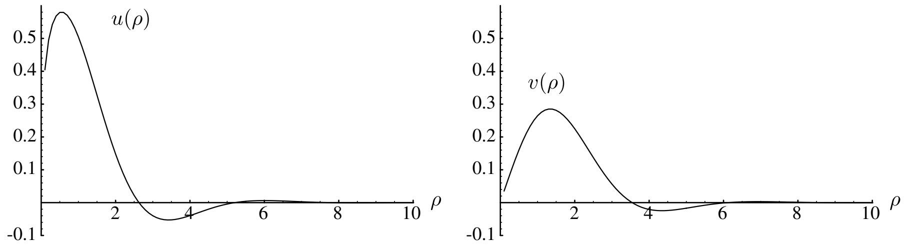

Fig. 2. The ρ dependence, in the equatorial plane ($z = 0$), of the lowest electronic wavefunction. Notice that this is a localized wavefunction. We show in (a) the wavefunction u, and in (b) the wavefunction v. In this paper we use dimensionless atomic units.

This form describes a magnetic flux equal to n flux quanta ($\Phi = n\phi_0 = n\frac{\hbar c}{2e}$). The wave functions u_i and v_i are expanded in a way similar to Ref. [31]

$$u_i(\mathbf{r}) = \sum_{\mu,j,k} c_{\mu,j,k}\phi_{j,\mu-n/2,k}\mathrm{e}^{\mathrm{i}(\mu-n/2)\varphi} \tag{10}$$

$$v_i(\mathbf{r}) = \sum_{\mu,j,k} \mathrm{d}_{\mu,j,k}\phi_{j,\mu+n/2,k}\mathrm{e}^{\mathrm{i}(\mu+n/2)\varphi} \tag{11}$$

where

$$\phi_{jmk} = \frac{\sqrt{2}}{RJ_{m+1}(\alpha_{jm})} J_m\left(\alpha_{jm}\frac{r}{R}\right)\frac{\mathrm{e}^{\mathrm{i}\frac{2\pi kz}{h}}}{\sqrt{h}} \tag{12}$$

Here μ is an half-odd integer if n is odd and an integer if n is even. J_m is a Bessel function. The system is placed in a cylinder of radius R and height h. Given the azimuthal symmetry of the system $\mathbf{A}$ does not depend on φ; therefore the Hamiltonian of the BdG equations may be simultaneously diagonalized for each value of μ. It is therefore enough to diagonalize the matrix

$$\begin{pmatrix} T^- & \Delta \\ \Delta^T & T^+ \end{pmatrix}\begin{pmatrix} c_i \\ d_i \end{pmatrix} = E_i\begin{pmatrix} c_i \\ d_i \end{pmatrix} \tag{13}$$

where

$$T^{\pm}_{jj'kk'} = \pm\frac{\hbar^2}{2m}\left(\alpha^2_{j\mu\pm n/2} + \frac{k^2\pi^2}{h^2}\right)\delta_{jj'}\delta_{kk'} - (\mu \pm n/2)\frac{\mathrm{e}}{\hbar c}I_1 \pm \frac{\mathrm{e}^2}{\hbar^2 c^2}I_2 - E_\mathrm{F} \tag{14}$$

with

$$I_1 = \int_0^h \mathrm{d}z \int_0^R \rho\mathrm{d}\rho\, \phi_{j,\mu\pm n/2,k}(\rho,z)\frac{A_\varphi(\rho,z)}{\rho}\phi_{j',\mu\pm n/2,k'}(\rho,z) \tag{15}$$

$$I_2 = \int_0^h \mathrm{d}z \int_0^R \rho\mathrm{d}\rho\, \phi_{j,\mu\pm n/2,k}(\rho,z)A_\varphi(\rho,z)^2\phi_{j',\mu\pm n/2,k'}(\rho,z) \tag{16}$$

We also obtain that

$$\Delta_{jj'kk'} = \int_0^h \mathrm{d}z \int_0^R \rho\mathrm{d}\rho\, \phi_{j,\mu-n/2,k}(\rho,z)\Delta(\rho,z)\phi_{j',\mu+n/2,k'}(\rho,z) \tag{17}$$

Notice that the main technical dificulty of the BdG aproach to the monopole–antimonopole confinement is the need to determine the full Fermi sphere of fermion wave-functions. In particular the deepest fermionic state for $n = 1$ is the one localized by the flux tube, depicted in Fig. 2. Because this state provides a finite contribution to the pairing function $\Delta(\mathbf{r})$, we cannot work with just a few states in the neighbourhood of the Fermi energy.

2.2. Monopole–antimonopole gauge field

In what concerns the vector gauge field $\mathbf{A}$, both in the BdG and in the Ginzburg–Landau approach, it is given by Maxwell's equations

$$\nabla \times \mathbf{B} = \nabla \times \nabla \times \mathbf{A} = \frac{4\pi}{c}\mathbf{J}, \tag{18}$$

which, in the Coulomb gauge ($\nabla.\mathbf{A} = 0$), is given by Poisson's equation,

$$\nabla^2 \mathbf{A} = -\frac{4\pi}{c}\mathbf{J}. \tag{19}$$

Thus, in superconductivity, the standard approximation is to solve classical equations for the gauge fields and only the fermions are quantized.

The vector potential has two contributions one due to the magnetic monopole–antimonopole, $\mathbf{A}^{\mathrm{ext}}$ and the other due to the currents that are formed in the superconductor, $\mathbf{A}^{\mathrm{sup}}$. Due to the linearity of the Maxwell equations we have that

$$\mathbf{A} = \mathbf{A}^{\mathrm{ext}} + \mathbf{A}^{\mathrm{sup}}, \tag{20}$$

and we use a similar decomposition for the currents and magnetic fields.

The current density originated in the supercurrents is obtained self-consistently by

$$\begin{aligned}\mathbf{J}^{\mathrm{sup}}(\mathbf{r}) = \frac{e\hbar}{\mathrm{i}m}\sum_i f(E_i)u_i^*(\mathbf{r})\left(\nabla - \frac{\mathrm{i}e}{\hbar c}\mathbf{A}(\mathbf{r})\right)u_i(\mathbf{r})\\ + (1 - f(E_i))v_i(\mathbf{r})\left(\nabla - \frac{\mathrm{i}e}{\hbar c}\mathbf{A}(\mathbf{r})\right)v_i^*(\mathbf{r}) - c\cdot c.\end{aligned} \tag{21}$$

To compute the contribution of the superconductor to the vector potential, we solve Poisson's equation,

$$\nabla^2 \mathbf{A}^{\mathrm{sup}} = -\frac{4\pi}{c}\mathbf{J}^{\mathrm{sup}}. \tag{22}$$

In what concerns the external monopole–antimonopole fields, the equation of Poisson does not need to be solved because the vector potential originated by a Dirac monopole, including a Dirac string, is well known. For instance the gauge field of a monopole located at the origin, with a vertical string at positive z is,

$$\mathbf{A}_1 = -\frac{g_{\mathrm{M}}}{4\pi}\frac{\rho}{r(r-z)}\mathbf{e}_\varphi \tag{23}$$

This form has a singularity on the line $(0,0,z)$ when $z \geqslant 0$, and it's curl reproduces the monopole and string magnetic field. This can be aplied to our choice for the geometric position of the monopole, antimonopole and respective Dirac Strings, discussed in detail in Section 1 and in Fig. 1. In this case we are interested in a situation where the currents of the two solenoids or magnetic whiskers inserted in the superconductor originate flux lines that penetrate the superconductor from the monopole and are recovered in the antimonopole. We consider one magnetic monopole located $-\mathbf{r}_0 = (0, 0, -z_0)$, and one magnetic antimonopole located at $\mathbf{r}_0 = (0, 0, z_0)$. The flux conservation is ensured by a vertical semi-infinite Dirac string linking $(0, 0, -\infty)$ to the monopole, and a second vertical semi-infinite string linking the antimonopole to $(0, 0, \infty)$, as in Fig. 1. Therefore we have singularities at $z > z_0$ and $z < -z_0$. The magnetic monopole and antimonopole produce the magnetic field

$$\begin{aligned}
\mathbf{B}^{\text{ext}} &= \mathbf{B}_1 + \mathbf{B}_2, \qquad (24)\\
\mathbf{B}_1 &= \frac{+g_{\text{M}}}{4\pi|\mathbf{r} + \mathbf{r}_0|^2}\widehat{r + r_0} + g_{\text{M}}\delta(x)\delta(y)\theta(-z - z_0)(\hat{e}_z),\\
\mathbf{B}_2 &= \frac{-g_{\text{M}}}{4\pi|\mathbf{r} - \mathbf{r}_0|^2}\widehat{r - r_0} - g_{\text{M}}\delta(x)\delta(y)\theta(z - z_0)(-\hat{e}_z),
\end{aligned}$$

where the string guarantees the conservation of magnetic flux $\nabla \cdot \mathbf{B} = 0$. The magnetic charge is equal to a quantum of magnetic flux,

$$g_{\text{M}} = \Phi_0 = \pi\frac{\hbar c}{|e|}. \qquad (25)$$

The gauge field created by the present monopole–antimonopole system has the form,

$$\mathbf{A}^{\text{ext}} = \frac{g_{\text{M}}}{4\pi}\left\{\frac{\rho}{|\mathbf{r} + \mathbf{r}_0|[|\mathbf{r} + \mathbf{r}_0| + (z + z_0)]} + \frac{\rho}{|\mathbf{r} - \mathbf{r}_0|[|\mathbf{r} - \mathbf{r}_0| - (z - z_0)]}\right\}\mathbf{e}_\varphi. \qquad (26)$$

With Eqs. (22) and (26) we may now compute the vector potential. Moreover we can verify that outside the Dirac strings, the fields do not depend on our choice of the Dirac string position [8]. Close to each Dirac string and far from the monopoles the external vector potential is approximately given by the infinite string vector potential

$$A_\varphi^{\text{ext}} = n_{\text{ext}}\frac{\hbar c}{2|e|\rho}, \qquad (27)$$

where, with our configuration, $n_{\text{ext}} = 1$. Then it can be shown [36] that the BdG equations can be recast in a form such that they only depend on the difference,

$$n_{\text{a}} = n - n_{\text{ext}} \qquad (28)$$

between the vorticity of the gap function (n) and the vorticity of the external line (n_{ext}). In the BdG equations we just have to replace $n \to n_{\text{a}}$ and the effect of the external infinitely thin solenoid is taken into account exactly if n_{ext} is an integer. In our geometric configuration for the Dirac strings, depicted if Fig. 1, it is easy to see that the effect of the strings is such that, in an approximate way, in the region $z < -z_0$ close to the string and far from the monopole, the BdG equations are approximately described by the equations where the effect of the external vector potential is equivalent to $n_a = 0$, since we choose $n = 1$ and the singular contribution from the string is described by $n_{\text{ext}} = 1$. A similar analysis for $z > z_0$ leads to the same conclusion. Between the monopoles a finite width flux tube forms. As shown in Ref. [36] these field lines are not singular and the vorticity of the equations is not affected: there is no string in this region. Therefore $n_{\text{a}} = n - n_{\text{ext}} = 1 - 0 = 1$. We can as well consider that the Dirac string has a finite extension and goes from the north monopole to the south monopole, as in the Ball and Caticha geometric configuration. In this case it is easy to see that the total flux is zero. It seems therefore natural to look for solutions where in our case $n = 1$ and in the Ball and Caticha case $n = 0$, reflecting the different total magnetic fluxes. The Ball and Caticha string configuration with $n = 0$ leads to a situation where for $z < -z_0$ and $z > z_0$ we have an effective $n_a = 0$ and between the monopoles we have $n_a = 1$. In this case there is a string between the monopoles (with $n_{ext} = -1$). Therefore the two configurations are equivalent as expected [8].

2.3. Numerical method

The BdG approach requires the full Fermi sphere of fermionic states. The wavefunctions are products of the different eigenvectors of the angular momenta L_z, the radial excitations expanded in a basis of cylindrical Bessel functions with a zero at the boundary, and the z axis functions expanded in trigonometric functions. We should note that we have to consider large systems and consequently a large basis of functions has to be used to properly obtain the exponential decay of the various physical quantities. Otherwise, the exponential regime is not reached. With, say 500 of each quantum number, we arrive at a set of the order of 10^8 different electronic wavefunctions in the smallest acceptable Fermi sphere. For instance the computation of the pairing function Δ and of the current $\mathbf{J}$ requires 3-dimensional integrals of the large 10^8 number of wavefunctions in the Fermi sphere. This also implies that solving the full 3d problem requires very large matrices to be diagonalized.

While solving the BdG equations in 2 dimensions is standard, see Ref. [36] for a recent example, in 3 dimensions an educated approximation is welcome, because we face the formidable task of diagonalizing 500 matrices of the order of $10^5 \times 10^5$, after the angular momentum is block diagonalized. Notice that the effective singularity of the topology and of the gauge fields is summarized in the number $n_a = n - n_{ext}$ [36]. Therefore we just add and subtract to the external vector potential the limiting singular expressions due to the strings. The remaining part of the vector potential is regular. It has been shown by several authors that in this case the contribution of the terms involving the regular part of the vector potential in the BdG equations is negligible or at least very small. We may therefore divide the system into two regions, using the inversion symmetry around $z = 0$. For $|z| < |z_0|$ we solve the BdG equations taking a basis with $n_a = 1$ (equivalent to the problem of a singly quantized vortex line with no external vector potential) and for $|z| > |z_0|$ we use a basis with $n_a = 0$. This allows us, in the following to neglect I_1 and I_2. We have to resort to this approximation for the z dependence.

In this approximation the eigenfunctions of the BdG Hamiltonian in each region are plane waves along z. Therefore the potential Δ does not depend on z and the BdG Hamiltonian is independent of z. It may be block diagonalized in terms of the momentum along the z direction (indexed by k). In this way the components of the Hamiltonian are reduced to

$$T^{\pm}_{jj'} = \pm \frac{\hbar^2}{2m}\left(\frac{\alpha^2_{j\mu\pm n_{a/2}}}{R^2} + \frac{4k^2\pi^2}{h^2}\right)\delta_{jj'} \mp E_F \tag{29}$$

$$\Delta_{jj'} = \int_0^R \phi_{j,\mu-n_{a/2}}(\rho)\,\Delta(\rho)\phi_{j',\mu+n_{a/2}}(\rho)\rho \mathrm{d}\rho \tag{30}$$

It is important to note that the symmetry of the BdG equations $u_i(\mathbf{r}) \rightarrow v_i^*(\mathbf{r})$, $v_i(\mathbf{r}) \rightarrow -u_i^*(\mathbf{r})$ and $E_i \rightarrow -E_i$ allows to reduce the solution to the positive values of μ. We obtain the eigenvectors and eigenvalues for negative values of μ using the above symmetry.

We may find the internal vector potential solving Poisson's equation,

$$\nabla^2 \mathbf{A}^{\text{sup}} = -\frac{4\pi}{c}\mathbf{J}^{\text{sup}}. \tag{31}$$

Defining its only component $A_\varphi^{\text{sup}} = F(\rho)/\rho$, Poisson's equation reduces in cylindrical coordinates to

$$\frac{\partial^2 F}{\partial \rho^2} - \frac{1}{\rho}\frac{\partial F}{\partial \rho} + \frac{\partial^2 F}{\partial z^2} = -\frac{4\pi}{c} J_\varphi \rho \tag{32}$$

Decomposing the current as

$$-\frac{4\pi}{c} J_\varphi \rho = K(\rho, z) + \beta(\rho, z) F(\rho, z) \tag{33}$$

with

$$K(\rho, z) = -\frac{4\pi}{c}\sum_i f(E_i)|u_i|^2(\mu - n_{\text{a}}/2) - (1 - f(E_i))|v_i|^2(\mu + n_a/2) \\ + \beta(\rho)(A^{\text{ext}} - A^{\text{sup}})\rho, \tag{34}$$

$$\beta(\rho) = -\frac{4\pi}{c}\frac{|e|}{\hbar c}\sum_i f(E_i)|u_i|^2 + (1 - f(E_i))|v_i|^2, \tag{35}$$

we get

$$\frac{\partial^2 F}{\partial \rho^2} - \frac{1}{\rho}\frac{\partial F}{\partial \rho} + \frac{\partial^2 F}{\partial z^2} = K(\rho, z) + \beta(\rho) F(\rho). \tag{36}$$

These equations may be solved as described in Ref. [36].

3. Results for $T = 0$

The parameters used are $\epsilon_{\text{F}} = 0.5$, $\omega_{\text{D}} = 0.25$, $g/\pi = 1$ in atomic units. We should note that the relevant parameter is the ratio to the critical temperature. For these parameters the critical temperature is of the order of 0.06. We consider the two monopoles in a system with height 960 and radius 480. The distance between the monopoles, d, is varied. Let us consider that the strings carry a quantum of flux.

In Fig. 3 we compare the absolute value of the total magnetic field for the cases of no superconductor, and in the superconducting phase considering a $n = 1$ solution and comparing to the case of $n = 0$. The case of no-superconductor is the usual magnetic dipole. Notice that the $n = 1$ and the $n = 0$ cases also correspond to two different configurations of confinement. The magnetic vortex provides a linear confining potential. In the $n = 1$ configuration the monopole is attracted by the antimonopole, this is the standard picture of confinement, say in a mesonic quark–anriquark system in QCD. In the $n = 0$ configuration the monopole is attracted by the boundary of the superconductor, not by the antimonopole. The $n = 0$ case simulates a situation where the magnetic solenoids are being

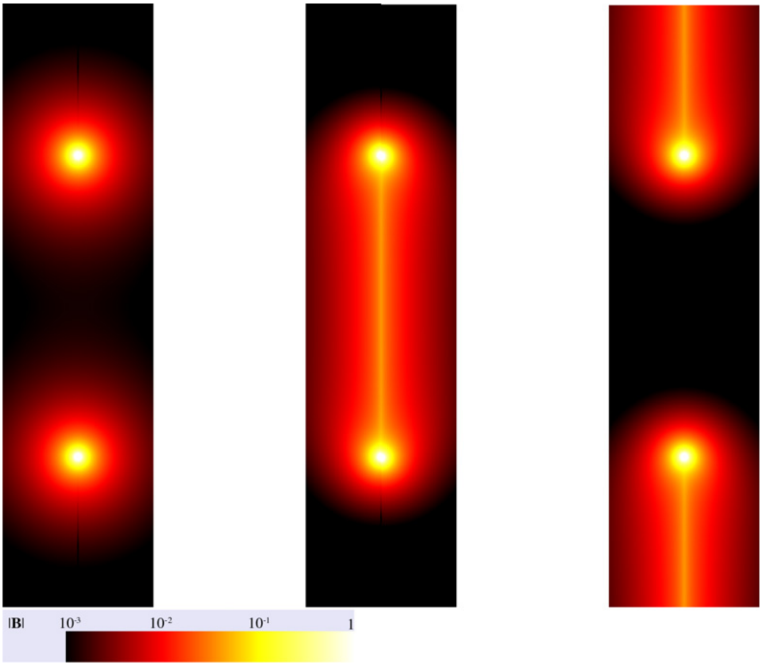

Fig. 3. Density plot for the total magnetic field $|\mathbf{B} = \mathbf{B}^{\text{ext}} + \mathbf{B}^{\text{sup}}|$ when the monopole and the antimonopole are separated by a distance $d = 2z_0 = 480$. The panels correspond from left to right to: no superconductor, superconductor with topological charge $n = 1$ and superconductor with topological charge $n = 0$, respectively.

inserted from the border of the material. When the solenoids are far enough, it is favourable for the flux lines to emerge from the material. As the monopoles get close together it is more favourable to establish a $n = 1$ flux tube between the monopoles.

Taking the solution of $n = 1$ we look for a solution where the flux is quantized and equal to a quantum of flux. Far from either monopole and close to the strings the magnetic field is small. In the case of $n = 0$ there is no flux through the system and the flux lines leave the superconductor from the monopoles to the border of the system. In Fig. 4 we show the total and internal magnetic fields for both $n = 1$ and $n = 0$. This figure provides complementary information with respect to Fig. 3. In the case of $n = 1$ the presence of the flux tube between the monopoles is evident. In the case of $n = 0$ the field lines avoid the central region except along the borders, as expected. The diamagnetic behaviour of the internal field, obtained subtracting the external field from the total field is clearly displayed in the right panels of Fig. 4. In the case of $n = 1$ the internal field close to the monopoles is not strong enough to compensate the external field. Note however that along the flux tube the internal field has the same orientation as the total field. Interestingly the internal field in the vicinity of the $z = 0$ region and far from the axis winds clockwise and counterclockwise. In the case of $n = 0$ once again along the flux tubes the internal field has the same orientation as the total field. Between the monopoles the internal field opposes the total field, as expected.

Clearly it is interesting, in the analogy of the Anderson–Higgs mechanism to the confinement of quarks, to determine the confinement potential between the two monopoles.

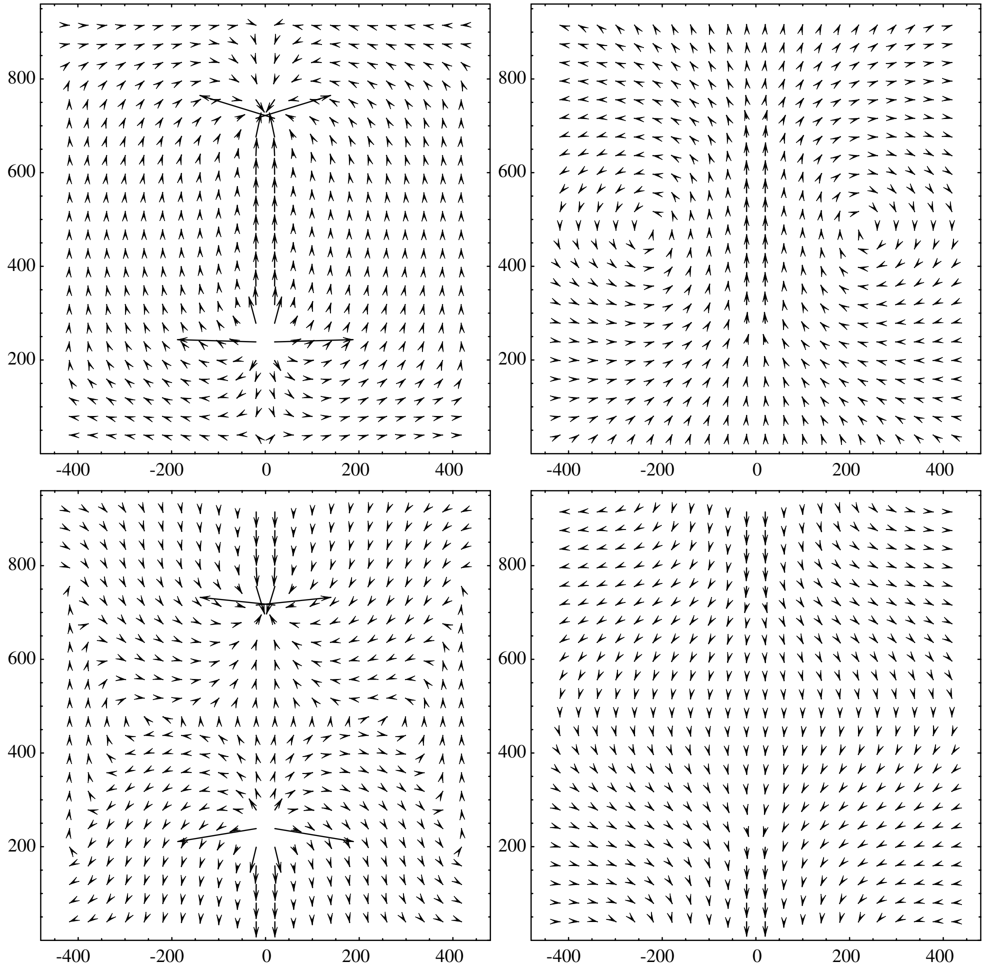

Fig. 4. Magnetic field profile for the total field (left panels) and the internal field (right panels). We consider the cases of $n = 1$ (upper panels) and $n = 0$ (lower panels). Please note that the magnitude of the field is not visible here when it is smaller than the size of the arrows. This information is contained in Fig. 3. The size of the arrows is chosen for better visualization of the field direction at each point.

Taking the analogy of the monopoles with the quarks in QCD the fact that these are linearly confined at large distances should translate in the superconductor to a linear potential energy when the monopoles are moved apart. Indeed in Fig. 5 we show the magnetic energy of the system,

$$U = \int \frac{|\mathbf{B}|^2}{8\pi} \mathrm{d}V, \tag{37}$$

as a function of the distance $d = 2\, z_0$ between the monopoles. The behaviour is similar to the one proposed for the confinement problem in QCD. In Fig. 5 we show the difference in energy between the normal system and the superconductor as a function of d. Interestingly, the solenoid–antisolenoid magnetic energy includes a subtle point. We do not in-

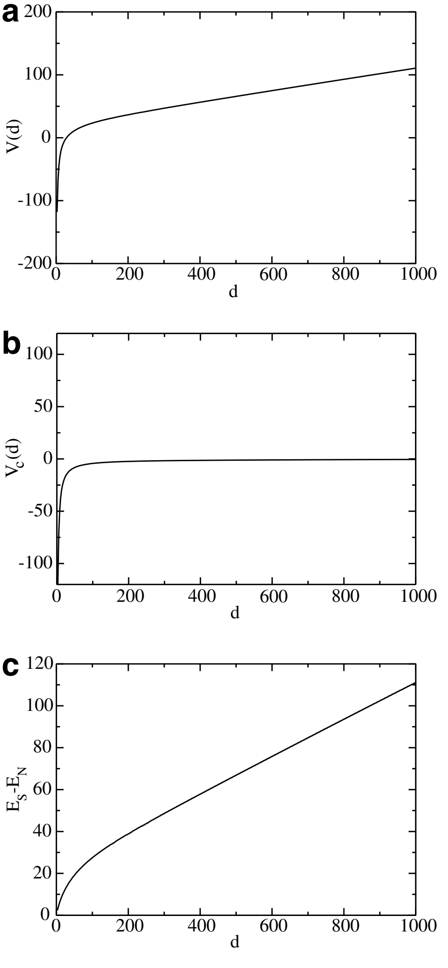

Fig. 5. (a) Total magnetic energy in the superconducting phase. (b) Total magnetic energy in the normal phase. (c) Energy difference between the superconductor and the normal phase. All energies are shown here as a function of the monopole–antimonopole distance $d = 2z_0$. In this paper we use dimensionless atomic units.

clude, for the computation of the magnetic energy, the magnetic field inside the Dirac strings. In the present case, the magnetization of both solenoids has to be maintained constant. We assume that this is an external task of the experimental apparatus. In the superconductor we obtain a linear potential at larger distances, as expected. The solenoid-antisolenoid magnetic force is attractive in the vacuum, the energy is simply a Coulomb term.

Indeed in Figs. 5a and b, we depict the magnetic energy of the solenoid-antisolenoid system both in the superconducting phase and in the normal phase (no superconductor). Although our solenoids are thinner than both the coherence length and the penetration length, they have a finite width, and we are able to account for the interior (string-like) magnetic field created by the solenoids. Notice that the $\frac{1}{r}$ component of the magnetic energy is decreasing. To isolate the linear potential we also shown in Fig. 5c the difference between the magnetic energy in the two phases. To get the monopole–antimonopole interaction, independently of the string internal energy, we also add to the linear interaction of Fig. 5a the monopole–antimonopole Coulomb interaction. This produces the potential depicted in 5a, similar to the linear + Coulomb potential of QCD.

4. Results for $T \neq 0$

In Figs. 6 and 7 we study the influence of temperature on the total field. As the temperature increases the flux tube between the two monopoles narrows in the intermediate region and close to the critical temperature, where the superconducting order vanishes, it approaches the normal phase regime where close to the monopoles the field intensity extends away from the axis. As the temperature increases the flux tubes narrow considerably until it breaks down when the superconductor becomes unstable and the system becomes normal. This happens both for $n = 1$ and $n = 0$. Again, the $n = 0$ case simulates a situation where the magnetic solenoids are being inserted from the border of the material such that it is favourable for the flux lines to emerge from the material. As the monopoles get closer it is more favourable to establish a flux tube between the monopoles.

We may consider different planes perpendicular to the string axis. The flux contained in any plane perpendicular to the strings axis is constant. In the regions far from the monopoles the flux is almost entirely contained in the strings. This is shown in Fig. 8. The flux profile is shown along a plane that intercepts the string and it is clear that the flux reaches its asymptotic value very close to the string. In the region between the monopoles the flux lines emerge and converge in the opposite charge monopole. In Fig. 8 it is clear that the flux grows smoothly from the origin, since in this case there is a considerable value of

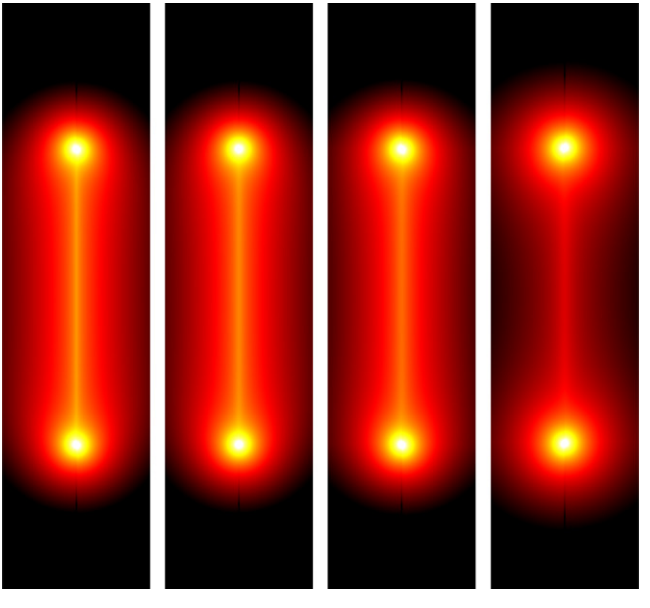

Fig. 6. Effect of temperature on the magnitude of the total magnetic field for $n = 1$. The temperatures are, from left to right, $T = 10^{-4}$, 0.02, 0.03, 0.04, respectively. For the density scale see Fig. 3.

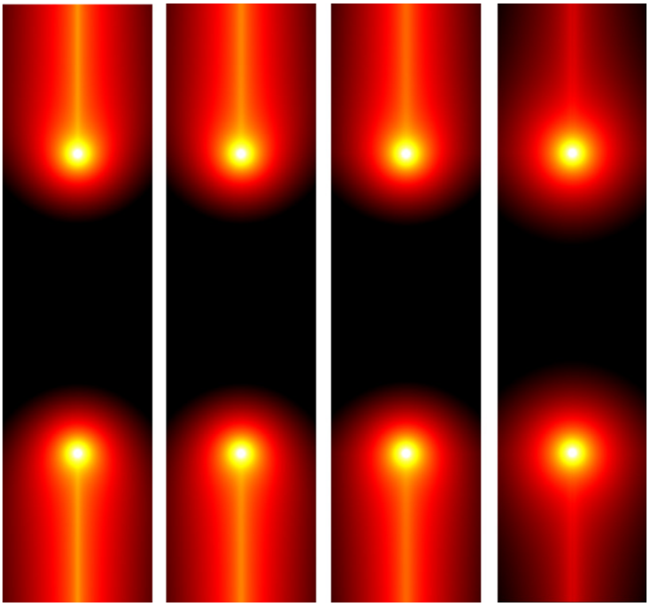

Fig. 7. Effect of temperature on the magnitude of the total magnetic field for $n = 0$. The temperatures are, from left to right, $T = 10^{-4}$, 0.02, 0.03, 0.04, respectively. For the density scale see Fig. 3.

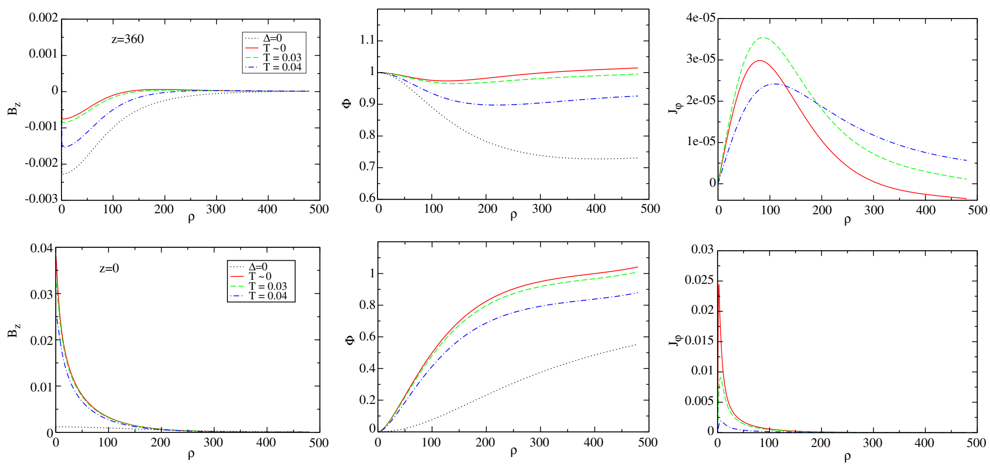

Fig. 8. Magnetic field, flux and current in the "tropics" ($z = 360$) above the north antimonopole, and in the equatorial plane ($z = 0$). The north antimonopole is at $z = 240$.

the magnetic field far from the axis. Also, we present results for B_z and J_φ also as a function of temperature.

In the central equatorial region ($z = 0$) the magnetic field is maximum on the axis and then decreases rapidly, on the scale of the penetration length. The field is compensated by the supercurrents that also decay rapidly as we move away from the axis.

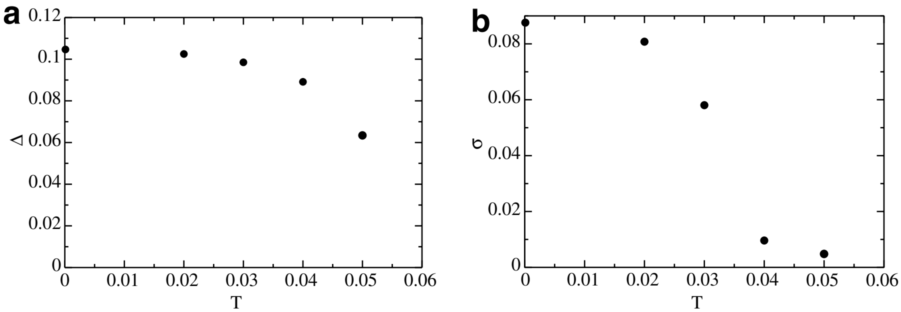

Fig. 9. (a) Order parameter Δ as a function of temperature, (b) String tension σ as a function of temperature.

In a plane such that we are already on the strings, the field is finite and negative at the axis but increases to zero far from the string. There is a cancellation between the field of the string and the field of the monopoles, as explained above. The supercurrents vanish on the string, then go through a maximum at a finite distance from the axis and then decrease far away. Note that the flux is already saturated on the axis, then decreases and the asymptotic value is recovered far from the axis.

As the temperature increases the penetration length increases. As a consequence both the increase and decrease of the field with distance sets on a larger scale as the temperature increases. This is clearly shown on the various quantities plotted in Fig. 8.

Finally, we consider in Fig. 9 the temperature dependence of the string tension. Also, we show the temperature dependence of the bulk value of the pairing function. We see that as the temperature increases both the pairing function and the string tension decrease, particularly as the critical temperature is approached. This critical temperature is defined as the temperature when the pairing function vanishes. Note that Fig. 9 shows that the string tension is already quite small when the pairing function is still finite, even though decreasing since the system is getting close to the critical temperature.

5. Conclusion

Motivated by the superconductor model for the confinement in QCD, we extended the Ball and Caticha work to include both the microscopic fermionic degrees of freedom of the superconductor and finite temperature. Our framework are the Bogoliubov-de Gennes equations solved in the external field lines of a monopole–antimonopole pair, including the associated semi-infinite magnetic strings. We address two confining configurations. In the common $n = 1$ configuration the monopole is attracted by the antimonopole. In the $n = 0$ configuration, equivalent to a case where one quark would try to eject itself from a quark–gluon plasma bubble into the confining vacuum, the monopole is attracted by the boundary of the superconductor, and thus is repelled to the outside of the superconductor.

Notice that this is not yet QCD, here we solve a condensed matter system. The advantage of studying a solenoid–antisolenoid pair in a superconductor is the more detailed nature of our results. For instance, we identify the well known localized fermionic states (unattainable via the Ginzburg–Landau approach [38]) important in the region where the supercurrents provide a topological charge. As expected in the Bogoliubov-de Gennes framework, we obtain one fermionic localized state per angular momentum [38]. Also, we analyze the dependence on the temperature of the string tension σ, of the fermion pairing order parameter Δ and of the magnetic topological flux Φ.

Nevertheless, this study is useful for the understanding of confinement and of temperature and density effects in QCD [39–50] or in Abelian QED [51,52]. These effects are usually explored with Lattice QCD or with Schwinger–Dyson equations. We note that the present framework can also be extended to model QCD. Importantly, this extension would be relevant to colour superconductivity, where the quark density is large, and to the quark-gluon plasma, where the temperature is finite.

We find that the magnetic field in the vortex, say in the equatorial plane for $n = 1$, decreases with increasing temperature. In what concerns the penetration length and the topological magnetic flux, it is seen from the results that the penetration length increases with temperature (as is well known), while the topological magnetic flux decreases for a specified distance. This decreases the string tension of the long distance monopole–antimonopole linear attraction. Notice that the string tension is already quite small when the pairing function is still finite, before it vanishes at the critical temperature. The quark–anriquark linear confining potential may suffer a similar decrease, before the temperature reaches the deconfinement temperature.

Acknowledgements

One of us (PDS) thanks the support of FCT under the grant POCTI/FIS/58133/2004.

References

[1] D.J. Gross, F. Wilczek, Phys. Rev. Lett. 30 (1973) 1343.
[2] H.D. Politzer, Phys. Rev. Lett. 30 (1973) 1346.
[3] H.B. Nielsen, P. Olesen, Nucl. Phys. B 61 (1973) 45.
[4] T. Goto, Prog. Theor. Phys. 46 (1971) 1560.
[5] Y. Nambu, Phys. Rev. D 10 (1974) 4262.
[6] G. 't Hooft, Nucl. Phys. B 79 (1974) 276.
[7] S. Mandelstam, Phys. Lett. B 53 (1975) 476.
[8] P.A.M. Dirac, Phys. Rev. 74 (1948) 817.
[9] M. Baker, J.S. Ball, F. Zachariasen, Phys. Rev. D 31 (1985) 2575.
[10] M. Baker, J.S. Ball, F. Zachariasen, Phys. Rept. 209 (1991) 73.
[11] K.G. Wilson, Phys. Rev. D 10 (1974) 2445.
[12] G.S. Bali, K. Schilling, Phys. Rev. D 46 (1992) 2636.
[13] G.S. Bali, K. Schilling, C. Schlichter, Phys. Rev. D 51 (1995) 5165.
[14] T.L. Ivanenko, A.V. Pochinsky, M.I. Polikarpov, Phys. Lett. B 252 (1990) 631.
[15] M.I. Polikarpov, A.I. Veselov, Nucl. Phys. B 297 (1988) 34.
[16] M.G. Alford, K. Rajagopal, F. Wilczek, Phys. Lett. B 422 (1998) 247.
[17] A. De Rujula, H. Georgi, S.L. Glashow, Phys. Rev. D 12 (1975) 147.
[18] A.B. Henriques, B.H. Kellett, R.G. Moorhouse, Phys. Lett. B 64 (1976) 85.
[19] T.T. Takahashi, H. Matsufuru, Y. Nemoto, H. Suganuma, Phys. Rev. Lett. 86 (2001) 18.
[20] T.T. Takahashi, H. Suganuma, Phys. Rev. Lett. 90 (2003) 182001.
[21] F. Okiharu, H. Suganuma, T.T. Takahashi, Phys. Rev. Lett. 94 (2005) 192001.
[22] F. Okiharu, H. Suganuma, T.T. Takahashi, Phys. Rev. D 72 (2005) 014505.
[23] A. Chodos, R.L. Jaffe, K. Johnson, C.B. Thorn, V.F. Weisskopf, Phys. Rev. D 9 (1974) 3471.
[24] R.L. Jaffe, K. Johnson, Phys. Lett. B 60 (1976) 201.
[25] P. Goddard, J. Goldstone, C. Rebbi, C.B. Thorn, Nucl. Phys. B 56 (1973) 109.
[26] P.J. d. Bicudo, J.E.F. Ribeiro, Phys. Rev. D 42 (1990) 1611.

[27] J.S. Ball, A. Caticha, Phys. Rev. D 37 (1988) 524.
[28] I.F. Lyuksyutov, D.G. Naugle, Mod. Phys. Lett. B 13 (1999) 491.
[29] V. Badri, A.M. Hermann, P. Lyman, in: B.V.R. Chowdari et al. (Eds.), Solid State Ionics: Science and Technology, World Scientific, Singapore, 1998, p. 441.
[30] C. Caroli, P.G. de Gennes, J. Matricon, Phys. Lett. 9 (1964) 307.
[31] F. Gygi, M. Schlüter, Phys. Rev. B 43 (1991) 7609.
[32] D. Rainer, J.A. Sauls, D. Waxman, Phys. Rev. B 54 (1996) 10094.
[33] P.G. de Gennes, Superconductivity of Metals and Alloys, Addison-Wesley, Reading, MA, 1989.
[34] I.F. Lyuksyutov, V. Pokrovsky, Mod. Phys. Lett. 14 (2000) 409.
[35] C. Berthod, Phys. Rev. B 71 (2005) 134513.
[36] M. Cardoso, P. Bicudo, P.D. Sacramento, J. Phys. Cond. Matt. 18 (2006) 8623.
[37] I.F. Lyuksyutov, V. Pokrovsky, Adv. Phys. 54 (2005) 67.
[38] S.M.M. Virtanen, M.M. Salomaa, Phys. Rev. B 60 (1999) 14581.
[39] T.A. DeGrand, C.E. DeTar, Nucl. Phys. B 225 (1983) 590.
[40] M. Teper, Phys. Lett. B 171 (1986) 81.
[41] C. DeTar, J.B. Kogut, Phys. Rev. Lett. 59 (1987) 399.
[42] S.A. Gottlieb, W. Liu, D. Toussaint, R.L. Renken, R.L. Sugar, Phys. Rev. Lett. 59 (1987) 2247.
[43] K.M. Bitar et al., Phys. Rev. D 43 (1991) 2396.
[44] A. Irback, P. LaCock, D. Miller, B. Petersson, T. Reisz, Nucl. Phys. B 363 (1991) 34.
[45] V. Koch, Phys. Rev. D 49 (1994) 6063.
[46] S. Ejiri, S.i. Kitahara, Y. Matsubara, T. Suzuki, Phys. Lett. B 343 (1995) 304.
[47] C. DeTar, Nucl. Phys. Proc. Suppl. 42 (1995) 73.
[48] H. Ichie, H. Suganuma, H. Toki, Phys. Rev. D 52 (1995) 2944.
[49] C.W. Bernard et al., Phys. Rev. Lett. 78 (1997) 598.
[50] C.W. Bernard et al., Phys. Rev. D 64 (2001) 074509.
[51] M.N. Chernodub, E.M. Ilgenfritz, A. Schiller, Phys. Rev. D 64 (2001) 054507.
[52] M.N. Chernodub, E.M. Ilgenfritz, A. Schiller, Phys. Rev. D 67 (2003) 034502.